Two Distinct Molecular Mechanisms Underlying Cytarabine Resistance in Human Leukemic Cells

Jie Cai,[1] Vijaya L. Damaraju,[2] Normand Groulx,[1] Delores Mowles,[2] Yunshan Peng,[3] Morris J. Robins,[3] Carol E. Cass,[2] and Philippe Gros[1]

[1]Department of Biochemistry, McGill University, Montreal, Quebec, Canada; [2]Department of Oncology, University of Alberta and Cross Cancer Institute, Edmonton, Alberta, Canada; and [3]Department of Chemistry and Biochemistry, Brigham Young University, Provo, Utah

Abstract

To understand the mechanism of cellular resistance to the nucleoside analogue cytarabine (1-β-D-arabinofuranosylcytosine, AraC), two resistant derivatives of the human leukemic line CCRF-CEM were obtained by stepwise selection in different concentrations of AraC. CEM/4×AraC cells showed low AraC resistance, whereas CEM/20×AraC cells showed high resistance. Both cell lines showed similar patterns of cross-resistance to multiple cytotoxic nucleoside analogues, with the exception that CEM/20×AraC cells remained sensitive to 5-fluorouridine and 2-deoxy-5-fluorouridine. Both cell lines were sensitive to 5-fluorouracil and to a variety of natural product drugs. Although both CEM/4×AraC and CEM/20×AraC cells displayed reduced intracellular accumulation of [^{3}H]AraC, only CEM/4×AraC cells showed reduced uptake of [^{3}H]uridine, which was used to assess nucleoside transport activities. Genes encoding proteins known to be involved in nucleoside transport, efflux, and metabolism were analyzed for the presence of mutations in the two cell lines. In CEM/4×AraC cells, independent mutations were identified at each allele of human equilibrative nucleoside transporter 1 (*hENT1*; *SLC29A1*), one corresponding to a single-nucleotide change in exon 4, the other being a complex intronic mutation disrupting splicing of exon 13. In contrast to CEM/20×AraC cells, CEM/4×AraC cells did not bind the hENT1/SLC29A1 ligand nitrobenzylmercaptopurine ribonucleoside and lacked detectable hENT1/SLC29A1 protein. In CEM/20×AraC cells, independent intronic mutations impairing splicing of exons 2 and 3 were found at each allele of the deoxycytidine kinase gene. These studies point to at least two distinct mechanisms of AraC resistance in leukemic cells. [Cancer Res 2008;68(7):2349–57]

Introduction

Cytarabine (1-β-D-arabinofuranosylcytosine, AraC) is a deoxycytidine analogue that has been used either alone or in combination with other chemotherapeutic agents for the treatment of acute myeloid leukemia (AML; refs. 1–3), relapsed and refractory acute lymphoblastic leukemia (ALL; refs. 4–6), and other malignancies (7–10). The chemotherapeutic efficacy of cytarabine varies dramatically between individuals. In general, standard induction therapy with combination of anthracycline and cytarabine produced 50% to 75% of complete remission rate in adult AML patients (1–3). Higher remission rate has been observed in newly diagnosed pediatric AML patients treated with improved chemotherapeutic regimens (11, 12). However, ~30% to 50% of patients relapse with drug resistant disease. Differences in genetic background, as well as efficiency of drug uptake, metabolism, and elimination may account for variable effectiveness of AraC-containing drug regimens.

Nucleoside analogue drugs, such as AraC and gemcitabine, have low rates of passive diffusion across membranes and enter cells primarily as fraudulent substrates for specialized nucleoside transporter proteins. Two distinct families of human nucleoside transporter proteins have been identified and characterized to date: the human equilibrative nucleoside transporters (hENT1–hENT4; also known as SLC29A1–SLC29A4) and the human concentrative nucleoside transporters (hCNT1–hCNT3; also known as SLC28A1–SLC28A3). hENT1/SLC29A1 has been shown to be the primary transporter responsible for cellular uptake of AraC (see refs. 13–17 for recent reviews). Once inside cells, AraC is "activated" to form AraCTP through sequential phosphorylation by deoxycytidine kinase (DCK), dCMP kinase, and nucleoside diphosphate kinase. The cytotoxicity of AraC is subsequently accomplished by nonproductive incorporation of AraCTP into nascent DNA or RNA. Decreased expression of *SLC29A1* mRNA and *DCK* mRNA is associated with reduced level of intracellular AraC uptake and reduced DCK activity, respectively; both alterations are associated with increased cellular resistance to AraC and gemcitabine in cancer cell lines (14–16, 18, 19). Although loss of *SLC29A1* gene function has yet to be described in AraC-resistant cells, numerous sequence polymorphisms (silent or missense variants) have been detected in the *SLC29A1* gene from different ethnic populations and have been speculated to contribute in part to the variable efficacy of AraC (20–22). On the other hand, overexpression of the gene encoding cytidine deaminase in transfected cells has been shown to cause increased AraC resistance, via deamination of AraC, the prodrug, to an inactive form (23–25). In addition, activation of 5′-nucleotidase and ribonucleotide reductase may affect conversion of AraC to the active inhibitor, possibly reducing its therapeutic efficacy (26–30). The overall efficacy of AraC as an anticancer drug may thus be modulated by a combination of factors, including variations in drug uptake, anabolic and catabolic pathways, as well as efflux activity (13, 17, 31–33).

In the present study, we used CCRF-CEM, an ALL cell line, as a cellular model to investigate molecular mechanisms underlying cellular resistance to AraC. Two cytarabine-resistant cell lines, CEM/4×AraC and CEM/20×AraC, were developed by continuous exposures and stepwise selection in increasing concentrations of AraC. The resistance phenotypes, the drug uptake properties, and the molecular mechanisms responsible for the observed drug

Note: Supplementary data for this article are available at Cancer Research Online (http://cancerres.aacrjournals.org/).

Requests for reprints: Philippe Gros, Department of Biochemistry, McGill University, 3655 Promenade Sir William Osler, Room 907, Montreal, Quebec H3G-1Y6, Canada. Phone: 514-398-7291; Fax: 514-398-2603; E-mail: philippe.gros@mcgill.ca.

doi:10.1158/0008-5472.CAN-07-5528

resistance were analyzed in the two resistant cell lines. Although derived from the same parental cell line, the two cell lines exhibited two distinct mechanisms of resistance to nucleoside analogue drugs.

Materials and Methods

Materials. AraC, 5-fluorouracil (5-FU), 5-fluorouridine, 5-fluoro-2-deoxyuridine, nitrobenzylmercaptopurine ribonucleoside (NBMPR), and dideoxycytidine were purchased from Sigma-Aldrich. Gemcitabine, Fludara, and Cladribine were obtained from the Hematology Department of Royal Victoria Hospital. [5-^{3}H]Uridine (19.3 Ci/mmol), [5-^{3}H]cytosine-β-D-arabinofuranoside ([^{3}H]AraC; 15-30 Ci/mmol), [^{3}H]NBMPR (15 Ci/mmol), and 2′-[^{3}H]deoxycytidine (27.7 Ci/mmol) were from Moravek Biochemicals. The anti-hENT1 monoclonal antibodies were developed and characterized previously (34) using synthetic peptides corresponding to amino acid residues 254 to 271 of hENT1/SLC29A1. 5′-*S*-{2-(1-[(fluorescein-5-yl)thioureido]-hexanamido)ethyl}-6-*N*-(4-nitrobenzyl)-5′-thioadenosine (FTH-SAENTA) is a fluorescein-tagged structural analogue of NBMPR that binds tightly to the transport-inhibitory sites of the hENT1/SLC29A1 protein (35) and, like SAENTA-FITC (36), can be used as a fluorescent probe to detect hENT1/SLC29A1 on cell surfaces. All other materials were of the highest available commercial grade.

Cell lines and culture conditions. Human CCRF-CEM (CEM, T-lymphoblastic leukemia) and HeLa cells were purchased from American Type Culture Collection. CEM/4×AraC and CEM/20×AraC were derived, respectively, by stepwise selection of CEM cells in the presence of AraC at concentrations equivalent to 4× and 20× its IC_{50} value for cytotoxicity against parental CEM cells. Clonal populations of CEM/4×AraC were isolated by limited dilution. RPMI 1640 and DMEM, supplemented with 10% fetal bovine serum, were used to grow CEM cells and HeLa cells, respectively. All cells were maintained at 37°C in a humidified air containing 5% CO_2. For CEM/4×AraC and CEM/20×AraC cells, AraC was added at the final concentrations used for selection.

Cytotoxicity assay. Cytotoxic effects of various drugs on CEM-resistant and AraC-resistant cells were assessed using a Trypan Blue dye exclusion assay. Briefly, cell suspensions (starting densities, 2×10^5 cells/mL) were cultured in the presence of graded concentrations of a drug of interest for 72 h. The viable cell counts were determined at various times by Trypan blue dye exclusion, and the growth rate for each condition was represented by the slope of the growth curve at exponential phase. The relative growth rate was obtained as a percentage of the growth rate of each cell line at a given drug concentration over that seen in the absence of drug. IC_{50} values correspond to drug concentrations that led to 50% reductions in cell growth rates compared with that in the absence of drug.

Preparation of total RNA and standard reverse transcription–PCR. Total cellular RNA was prepared from exponentially growing CEM, CEM/4×AraC, and CEM/20×AraC cells using Tri Reagent (Sigma-Aldrich) after the manufacturer's instructions. Reverse transcription reactions using total RNA were carried out with random hexamer oligos using M-MuLV reverse transcriptase (New England Biolabs) following the manufacturer's instructions. Gene-specific PCR amplification (reverse transcription–PCR, RT-PCR) was performed for 25 to 30 cycles using Platinum Taq DNA polymerase high fidelity (Invitrogen) under experimental conditions suggested by the supplier. Gene-specific oligonucleotides used to amplify individual cDNA fragments are listed in Supplementary Table S1. The specificity and purity of individual RT-PCR products was ascertained by agarose gel electrophoresis before cloning and/or DNA sequencing.

Cloning and sequencing of human *SLC29A1* and *DCK1* cDNAs and genomic segments. The oligonucleotides used in RT-PCR to generate a full-length cDNA for *SLC29A1* were SLC29A1-F1, 5′-A*GCTAGCAGATCT*ATCACCATGACAACC AGTCACCA-3′, and SLC29A1-R2, 5′-*CTCTAGA*CACAATTGCCCGGAACAGGAA-3′, which includes restriction enzyme sites used for subcloning (in italics). *SLC29A1* cDNA products were cloned in a plasmid vector (TOPO cloning kit; Invitrogen). Similarly, full-length *hDCK* cDNAs were generated using oligonucleotides hDCK-F1 (5′-*AGATCT*ATGGC CACCCCGCCCAAGA-3′) and hDCK-R2 (5′-*TCTAGA* CAAAGTACTCAAAAACTCTTTGAC-3′). Twenty-four cDNA clones from each transformation were expanded, and their DNA sequences were determined. Sequencing data alignment analysis was performed using BioEdit software.

Alterations detected in cDNA clones of *SLC29A1* and *DCK1* were validated at the genomic level by PCR amplification and sequencing of the corresponding gene exons (E) and introns (I). PCR fragments corresponding to I3-E4 and E12-I12-E13 of the *SLC29A1* gene and I1-E2 and I2-E3 regions of *DCK* were obtained using gene-specific oligonucleotide primer pairs, including SLC29A1-IN3F/SLC29A1-IN4R (5′-TAGAGAGACT-GACAACGGACAG-3′/5′-TGCAAGCACAGTGGGCACT-3′), SLC29A1-IN11F/SLC29A1-IN13R (5′-TGCCTCTGTGAGCCTGATAA-3′/5′-AACTC TAGAT-CCTGTCTGATG-3′) and DCK-In1F/DCK-In2R (5′-GTAAATCTTGCAAAAG CTAATG-3′/5′-GAAGATATATACCTAAAGCGAGAT-3′), DCK-In2F/DCK-In3R (5′-TTGCTGATCATGATTACATTTATTT-3′/5′-ATGGCCACGTA-CAAGCC AT-3′). The PCR products were then purified, and their sequences were determined using Thermo sequenase radiolabeled terminator cycle sequencing kit (U.S. Biochemical Corporation). The sequencing reactions were resolved on 8% polyacrylamide gels followed by autoradiography. For the *SLC29A1* E12-I12-E13 and *DCK* I2-E3 regions, PCR amplicons were cloned in TOPO vector, and individual clones were sequenced to verify mutations on individual alleles.

Transfection of human *SLC29A1* cDNA into HeLa cells. A wild-type full-length *hENT1/SLC29A1* cDNA (from CEM) cloned in TOPO vector was further subcloned into the mammalian expression vector pcDNA6-V_5-HisA (Invitrogen) and transiently transfected into HeLa cells using Lipofectamine 2000 (Invitrogen) following the manufacturer's instructions. The "empty" pcDNA6-V_5-HisA vector was also transfected into HeLa cells as a negative control. For immunoblotting, cells were trypsinized, collected by centrifugation, and washed with PBS. Crude membrane fractions and whole-cell extracts were prepared and separated by SDS-PAGE. Immunodetection of the hENT1/SLC29A1 protein was carried out using a monoclonal anti-ENT1 antibody preparation.

Cell surface staining using FTH-SAENTA. The cell surface abundance of hENT1/SLC29A1 in different CEM cells was determined using FTH-SAENTA, a membrane-impermeable NBMPR analogue. Briefly, cells washed free of media were resuspended in PBS to $\sim 10^5$ cells/mL and incubated with either 0, 100 nmol/L FTH-SAENTA, or 100 nmol/L FTH-SAENTA + 10 μmol/L NBMPR (cells were preincubated with NBMPR for 10 min before addition of FTH-SAENTA) for 1 h at room temperature. Cells were then centrifuged, washed once quickly, and, in a small volume of PBS, placed on polylysine-coated dishes to attach for visualization by confocal microscopy. For fluorescence-activated cell sorting (FACS) analysis of cell surface binding of FTH-SAENTA, cells were washed free of growth medium and resuspended in sodium buffer (144 mmol/L NaCl, 20 mmol/L Tris, 3 mmol/L K_2HPO_4, 1 mmol/L $MgCl_2$, 1.4 mmol/L $CaCl_2$, and 5 mmol/L glucose at pH 7.4) to a final cell density of 2.5×10^5 cells/mL. Cells were treated at room temperature for 1 h with either no compound (negative control), 100 nmol/L FTH-SAENTA, or 100 nmol/L FTH-SAENTA + 10 μmol/L NBMPR. At the end of 1 h, cells were collected by centrifugation and washed twice with sodium buffer. The cells were analyzed for fluorescence using a BD Flowcytometer.

Analysis of cell surface hENT1/SLC29A1 sites by [^{3}H]NBMPR binding. Cell surface abundance of hENT1/SLC29A1 on CEM and CEM-AraC cells was assessed by equilibrium binding studies with 10 nmol/L [^{3}H]NBMPR. Cells were washed free of medium, and cell suspensions containing 10^6 cells in 100 μL of sodium buffer were incubated with 10 nmol/L [^{3}H]NBMPR in the absence or presence of 100 nmol/L FTH-SAENTA or 10 μmol/L unlabeled NBMPR at room temperature for 1 h. At the end of the incubation, cells in permeant mixture were centrifuged through oil (4:1 v/v of silicon oil/mineral oil) to remove free unbound [^{3}H]NBMPR. The cell pellet was solubilized in 5% Triton X-100 and counted in a Beckman scintillation counter.

Measurement of [^{3}H]AraC uptake. Assays of [^{3}H]AraC uptake were conducted in PBS containing 10 mmol/L glucose and 2 mmol/L glutamine (PBS/GG) at 37°C. Briefly, 10^6 exponentially growing cells were collected, washed once with PBS, and resuspended in 500 μL of PBS/GG for 15 min,

after which [^{3}H]AraC (final concentration, 200 nmol/L) was added and the reaction mixtures were incubated for 30 min. Each reaction mixture was then gently transferred to a prewarmed microcentrifuge tube containing 200 μL of oil cushion (see above), followed by centrifugation at 8,000 × *g* for 30 s. After removing supernatants, the cell pellets were washed twice with PBS, digested with 100 μL of 1 N NaOH, and neutralized by addition of 100 μL of 1 N HCl. The cell-associated radioactivity was measured by liquid scintillation counting. For assays under ATP depletion conditions, PBS was used instead of PBS/GG buffer, and cell suspensions were preincubated with rotenone (20 ng/mL) for 15 min and then 2-deoxyglucose (2 mmol/L) for another 15 min before the addition of [^{3}H]AraC.

DCK activity assay. DCK activity was determined as described (18) with minor modifications. Briefly, 4 × 10^6 cells (per reaction) were collected, washed twice with PBS, and lysed in 100 μL of CelLytic M (Sigma) following the manufacturer's instructions. Cell lysates were clarified by centrifugation at 20,000 × *g* for 10 min and used either immediately for DCK assays or stored at −70°C. DCK activity was measured in reaction mixtures containing 10 μmol/L [^{3}H]deoxycytidine, 5 mmol/L ATP, 5 mmol/L $MgCl_2$, 50 mmol/L Tris-HCl (pH 7.5), 10 mmol/L NaF, 2 mmol/L DTT, and 1.8 mmol/L thymidine (buffer A). Reactions were started by addition of 5 μL of cell lysate to 500 μL of prewarmed buffer A (for 5 min) at 37 °C. For time courses, 100-μL samples were pipetted onto Whatman DE-81 filter discs fitted to a vacuum device. Filters were then washed thrice with 5 mL of cold water each time and air-dried, and the radioactivity on the filters was measured by liquid scintillation counting. Each experiment was repeated at least thrice.

Results

Development of AraC-resistant CCRF-CEM cell lines. A stepwise selection protocol in drug-containing medium was used to derive AraC-resistant CEM cell lines. The IC_{50} value of CEM cells for AraC was 0.025 μmol/L. CEM cells were initially passaged in small increments of AraC concentrations above this IC_{50}, leading after several months to the isolation of a subpopulation of CEM cells that retained excellent growth rates in 0.1 μmol/L AraC and were designated CEM/4×AraC. Further stepwise selection of this cell population in AraC concentrations up to 20× the IC_{50} value resulted in the isolation of a second population of AraC-resistant cells, CEM/20×AraC. Both CEM/4×AraC and CEM/20×AraC cells showed no visible morphologic and size differences from their parental CEM cells. Cytotoxicity assays showed that both CEM/4×AraC-resistant and CEM/20×AraC-resistant cell lines were highly resistant to AraC compared with parental CEM cells, with

A

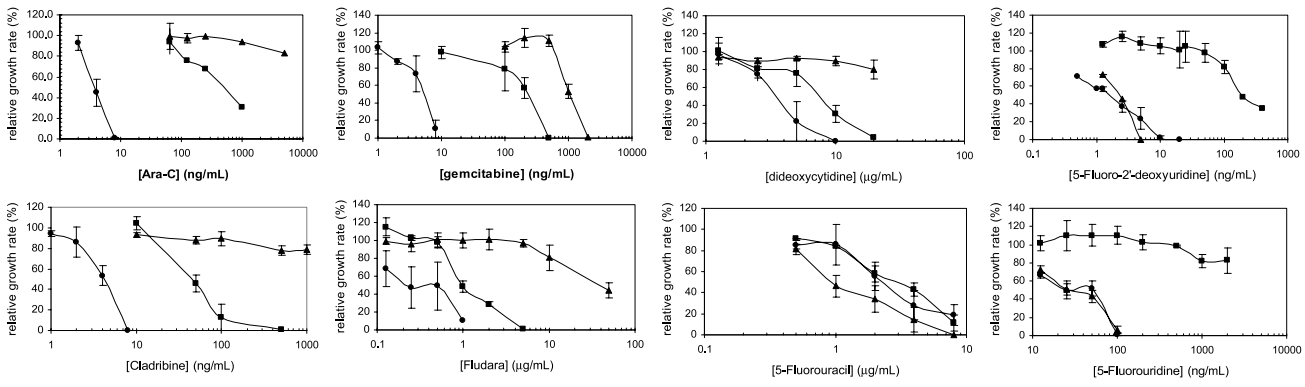

B

Drugs	Cytotoxicity (IC_{50}, ng/mL)			Relative resistance (fold)	
	CEM	4xAraC	20xAraC	4xAraC	20xAraC
Cytarabine	4	500	>1000	125	>250
Gemcitabine	5.5	220	1050	40	191
Cladribine	4.2	40	>1000	9.5	>250
Fludara	250	2500	35000	10	117
Dideoxycytidine	3500	7000	>20000	2	>8
5-Fluoro-2'-deoxyuridine	2	200	2.2	100	1.1
5-Fluorouridine	25	>2000	25	>80	1
5-Fluorouracil	2.5	4	1	1.6	0.4
Daunorubicin	4.2	3.2	N.D.	0.76	N.D.
Etoposide	55	55	N.D.	1	N.D.

Figure 1. Drug resistance profiles of CEM (●), CEM/4×AraC (■), and CEM/20×AraC (▲) cells. *A,* proliferating cell cultures were exposed to increasing concentrations of various drugs as indicated. Cell viability was determined over time by Trypan blue dye exclusion as described. Relative cell growth rate (in percentage) was expressed as the function of drug concentration. *Points,* mean of at least three independent experiments; *bars,* SE. *B,* summary of cytotoxicity of various drugs by comparing IC_{50} values of each drug on individual cell lines. The IC_{50} values were defined as described in Materials and Methods and deduced from *A. N.D.,* not determined.

increases in their IC_{50} values of 125-fold and >200-fold, respectively (Fig. 1). Further drug resistance profiling analysis revealed that both cell lines were cross-resistant to several nucleoside drugs, including Gemcitabine, Cladribine, Fludara, and dideoxycytidine, with higher levels of resistance observed in the CEM/20×AraC cells. However, the two cell lines differed markedly in their degree of resistance to 5-fluorouridine and 5-fluoro-2′-deoxyuridine, with CEM/4×AraC being resistant to both compounds, whereas CEM/20×AraC remained as sensitive as the parental CEM cells. These differences in drug resistance profiles suggested a distinct mechanistic basis in the two cell populations. Both CEM/4×AraC and CEM/20×AraC remained sensitive to 5-FU (Fig. 1) and to a variety of natural products, including anthracyclines and etoposide (Fig. 1*B*). The lack of cross-resistance to natural products suggested that ABC transporters, such as ABCB1 (MDR1/P-glycoprotein) and multidrug resistance associated protein ABCC1 (MRP1), were not responsible for the resistance of these cells.

Expression of candidate genes in AraC-resistant CEM cells. To gain insight into possible mechanisms responsible for drug resistance in CEM/4×AraC and CEM/20×AraC cells, expression of mRNAs corresponding to several candidate genes known to be involved in transport and/or metabolism of nucleoside analogue drugs was investigated by RT-PCR. These genes encoded nucleoside transporters (SLC29A1 and A2, SLC28A1 and A2), ATP-dependent efflux pumps (ABCC4 and 5), and enzymes known to be involved in drug metabolism, such as DCK, cytidine deaminase (CDADC1), and ribonucleoside reductase large subunit (RRMI). These analyses failed to detect major differences in expression levels or sizes of cDNAs produced by the resistant isolates, with two notable exceptions. CEM/4×AraC cells expressed what seemed to be an altered *SLC29A1* mRNA compared with both CEM (Fig. 2) and CEM/20×AraC (data not shown) cells. Using a primer pair (F1 and R3) designed to amplify the entire coding region of the *SLC29A1* mRNA, CEM/4×AraC cells displayed a wild-type product similar in length to that detected in the parental cells (1380 bp) but also showed a shorter fragment of ~1,260 bp (Fig. 2). Further RT-PCR studies with other primer pairs consisting of F1 as an anchor primer (exon 3) and other primers spanning different portions of the *SLC29A1* cDNA showed that the altered product was only detected with exon 14–derived primers (F1 + R3) and not with further upstream primers, including one from exon 13 (F1 + R2). This suggested a possible deletion in the cDNA sequence derived from the exon 13 region in one or both copies of the *SLC29A1* gene in CEM/4×AraC cells. No such alterations were noted in CEM/20×AraC cells.

Genetic lesions in the *SLC29A1* gene from CEM/4×AraC cells. To delineate the nature of possible mutations found in *SLC29A1* from CEM/4×AraC cells, the amplified RT-PCR products were cloned and sequenced. Two mutations were found in *SLC29A1* cDNAs from CEM/4×AraC cells (Fig. 3*A*). A nonsense mutation was detected at the beginning of exon 4 at the Tyr^{11} codon (TA*C*→TA*A*), resulting in a termination codon. The second mutation was the complete absence of exon 13 in some of the clones, consistent with the size differences in cDNA products from CEM/4×AraC detected in Fig. 2. Importantly, individual cDNA clones were found to contain either type of mutation, but not both, suggesting that the two alterations corresponded to different genetic lesions on each of the two alleles of the *SLC29A1* gene in CEM/4×AraC cells. The mutations detected by cDNA sequencing were further validated by characterization of the corresponding genomic regions in the *SLC29A1* gene, which were amplified by PCR and sequenced with [^{33}P]dATP (autoradiograms shown in Fig. 3*B* and *C*). These experiments validated the presence of a heterozygote nonsense mutation at the genetic codon for Tyr^{11} of *SLC29A1* in genomic DNA from CEM/4×AraC cells (Fig. 3*B*). Additionally, a complex pattern of sequence alterations was noted in a 15-nucleotide segment overlapping the exon 13/intron 13 junction of the *SLC29A1* gene (Fig. 3*C*), including an alteration in the 5′ splice sequence (*GU*GAGU→GGGGGU) in intron 13 and a single-nucleotide deletion in the 3′ end of exon 13 (Fig. 3*C*). This complex mutation was verified by cloning the PCR products followed by DNA sequencing (Fig. 3*C, right*) and was, therefore, very likely to account for the altered splicing of exon 13 detected by cDNA sequencing from CEM/4×AraC RNA. That both types of

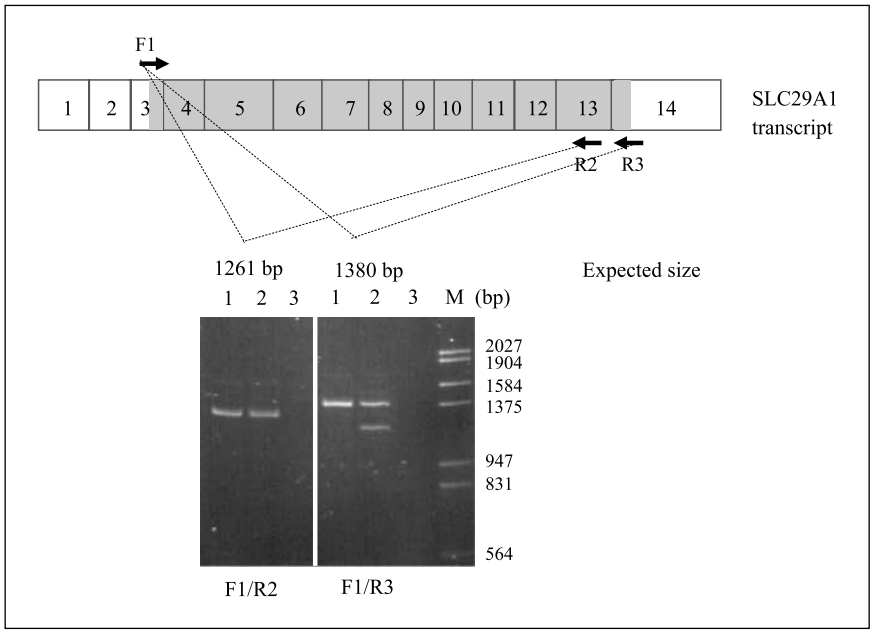

Figure 2. Standard RT-PCR of the *SLC29A1* gene from CEM (*lane 1*) and CEM/4×AraC (*lane 2*) cells, using two pairs of oligonucleotides. The top bar graph shows the schematic representation of the SLC29A1 transcript with the exons numbered and the coding region shaded. F1, R2, and R3 indicate forward and reverse oligonucleotides, respectively. *Arrows,* orientation and relative positions of the oligonucleotides in the transcript sequence. The left panel of the RT-PCR gel picture shows the SLC29A1 cDNA obtained using primer pair F1/R2, and the right panel shows the SLC29A1 cDNA products obtained using primer pair F1/R3. *Lane 3,* negative control with primers only; *lane M,* a size marker. The drawing of the SLC29A1 transcript is not to scale.

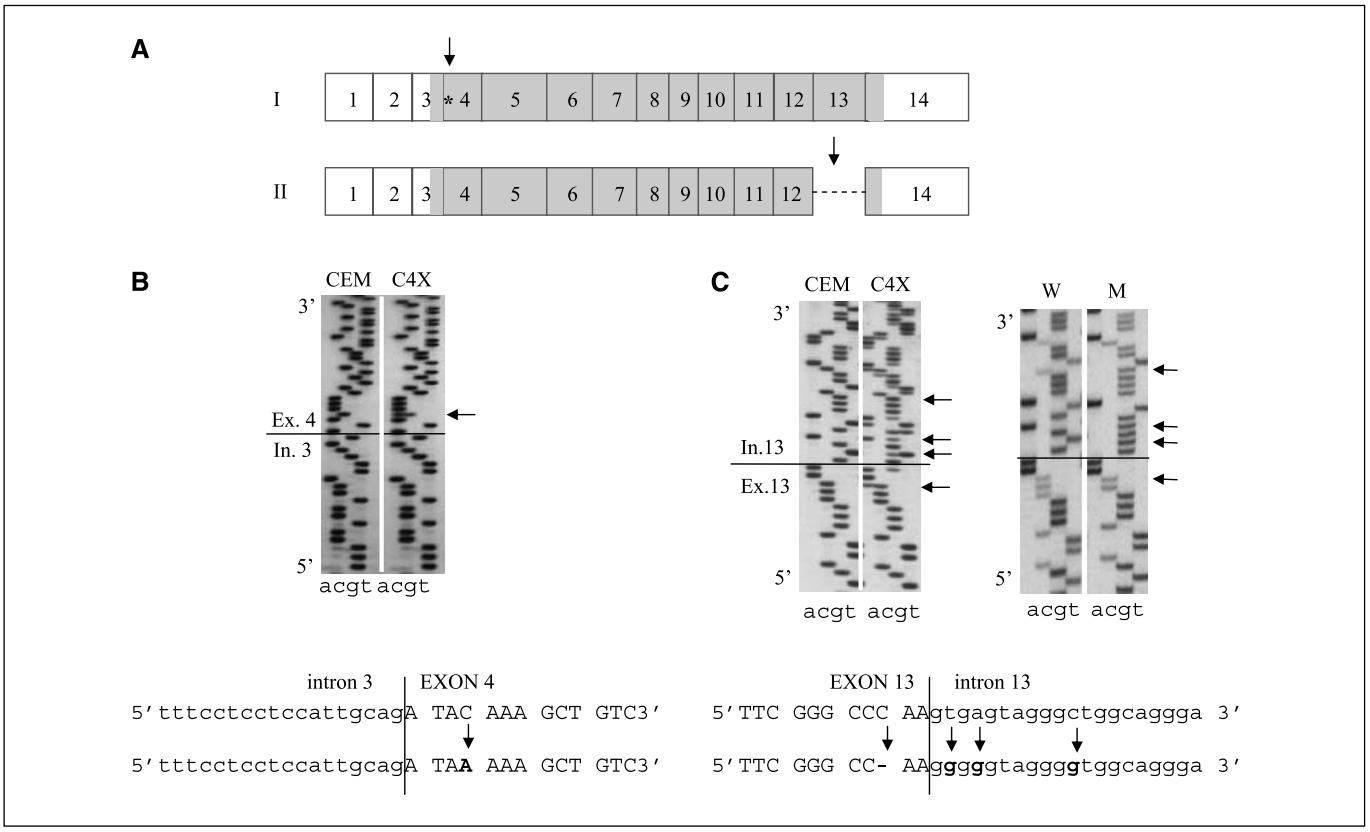

Figure 3. Identification of the *SLC29A1* mutations in CEM/4×AraC cells. *A,* schematic representation of two major types of mutations found in cloned full-length coding cDNA from CEM/4×AraC. *Type I,* a (c to a) single-nucleotide change that leads to the change of amino acid Tyr[11] (tac) to a STOP codon (taa; *top*). *Type II,* a deletion of the entire exon 13, represented by dashed line (*bottom*). The numbers represent exons, and the shading represents coding regions. *B,* autoradiograph of [^{33}P]dATP labeled DNA sequencing gel (*top*) and the deduced DNA sequences (*bottom*) of the SLC29A1 genomic DNA from CEM (*left*) and CEM/4×AraC (*right*), respectively, in the region of type I mutation. *C,* autoradiograph of [^{33}P]dATP labeled DNA sequencing gels (*top*) and their deduced DNA sequences (*bottom*) of the SLC29A1 genomic DNA from CEM and CEM/4×AraC, respectively, in the region of type II mutation. *Left,* sequencing gel of direct genomic PCR products; *right,* sequencing gel of cloned genomic PCR products. *W,* wild-type allele; *M,* mutant allele. The positions of mutated residues are indicated by arrows. Boundaries between intron and exons are indicated by lines.

mutations were present as heterozygotes in genomic DNA confirmed results from cDNA sequencing and established that both alleles of the *SLC29A1* gene in CEM/4×AraC were null alleles likely to encode nonfunctional proteins resulting in the absence of nucleoside transport activity. These data strongly suggest that mutations in the *SLC29A1* gene were responsible for the observed drug resistance in CEM/4×AraC cells.

Lack of hENT1/SLC29A1 protein in CEM/4×AraC cells. To validate the predicted effect of *SLC29A1* gene mutations on protein expression, whole-cell extracts and crude membrane fractions were prepared from CEM/4×AraC and parental CEM cells and analyzed by immunoblotting with anti-hENT1/SLC29A1 antibodies (Fig. 4*A*). In these experiments, HeLa cells transiently expressing a full-length *SLC29A1* cDNA were used as positive controls. Although an immunoreactive species of predicted molecular mass ~60 kDa was detected in extracts from CEM and HeLa/SLC29A1 transfectants, this species was undetectable in CEM/4×AraC cells (Fig. 4*A*). The absence of hENT1/SLC29A1 protein in CEM/4×AraC cells was further validated by the lack of fluorescent staining of isolated CEM/4×AraC clones incubated with FTH-SAENTA, a fluorescent probe known to specifically bind to cell surface hENT1/SLC29A1 protein, and detectable by confocal microscopy (Fig. 4*B*). Further quantification of hENT1/SLC29A1 protein expression using FTH-SAENTA staining followed by FACS analysis was conducted (Fig. 4*C*). Specific binding of FTH-SAENTA to parental CEM cells was shown by the complete inhibition of binding by preincubation of cells with the hENT1/SLC29A1-specific inhibitor, NBMPR (Fig. 4*C, top*). Similar analysis of an isolated CEM/4×AraC clone revealed no such fluorescent labeling on the cell surface in the absence of NBMPR (Fig. 4*C, middle*). Three additional CEM/4×AraC clones produced similar results (data not shown). Finally, results from additional [^{3}H]NBMPR binding studies were consistent with those of the fluorescence labeling studies and showed binding of the probe to parental CEM cells (competable by FTH-SAENTA or unlabeled NBMPR) but not to a CEM/4×AraC cell clone (Fig. 4*D*). Taken together, the defects in the *SLC29A1* gene of CEM/4×AraC cells abolished cell surface expression of the hENT1/SLC29A1 protein in this drug-resistant cell population.

Drug uptake in CEM/4×AraC and CEM/20×AraC cells. CEM cells possess a single type of nucleoside transporter, hENT1/SLC29A1 (37). The mutations in *SLC29A1* found in CEM/4×AraC cells may have impaired nucleoside transport, causing reduced cellular accumulation and increased resistance to cytotoxic nucleoside drugs, including AraC. Therefore, uptake of [^{3}H]AraC was measured in CEM, CEM/4×AraC, and CEM/20AraC cells. Results in Fig. 5*A* showed that neither CEM/4×AraC nor CEM/20×AraC cells accumulated [^{3}H]AraC. This was consistent with mutations in the *SLC29A1* gene of CEM/4×AraC cells but

surprising for CEM/20×AraC cells, which did not harbor such mutations and seemingly exhibited hENT1/SLC29A1 on their surfaces (Fig. 4*B* and *C, bottom*). Reduced drug uptake in both resistant cell lines was not affected by ATP depletion (Fig. 5*A*), suggesting that the reduced intracellular accumulation of [^{3}H]AraC in the CEM/20×AraC cells was not caused by defects in unrelated ATP-dependent drug uptake or drug efflux mechanisms. Further transport studies using the normal physiologic nucleoside substrate [^{3}H]uridine showed that both CEM and CEM/20×AraC cells accumulated uridine at similar levels, whereas CEM/4×AraC cells showed no accumulation of this nucleoside (data not shown). These results confirmed that the CEM/4×AraC cells were "null" for nucleoside import by hENT1/SLC29A1. On the other hand, CEM/20×AraC seemed to possess normal nucleoside transport activity (cell surface expression, transport of [^{3}H]uridine), although they were highly resistant to cytotoxic concentrations of AraC and did not accumulate [^{3}H]AraC in uptake assays.

An alternative drug resistance mechanism in the CEM/20×AraC cells. Because CEM/20×AraC cells did not harbor mutations in the *SLC29A1* gene, exhibited hENT1/SLC29A1 on their surface, and could import [^{3}H]uridine, additional candidate genes were investigated. DCK is responsible for the first modification required for metabolism of AraC. The kinase activity of DCK was assayed in CEM, CEM/4×AraC, and CEM/20×AraC cells. Although robust DCK activity was detected in CEM and CEM/4×AraC cells, it was largely absent in CEM/20×AraC cells (Fig. 5*B*). Cloning and sequencing the *DCK* cDNA from RNA of the CEM/20×AraC cells revealed two mutations (Fig. 6*A*). The first corresponded to a deletion of the first six nucleotides in exon 2, whereas the second was an insertion of 22 nucleotides at the exon 2 and exon 3 junction (Fig. 6*A*). To validate the mutations detected in cDNA clones from *DCK* of CEM/20×AraC cells, genomic DNA fragments overlapping the exon-intron junctions of intron 1 and exon 2, intron 2 and exon 3 were PCR-amplified, followed by cloning and nucleotide sequencing. A single-nucleotide substitution (a→c) was identified at the splice junction of intron 1 and exon 2 (Fig. 6*B*). This mutation was heterozygous and was likely responsible for the inappropriate splicing of intron 1, including deletion of some exon 2 sequence in the resulting mRNA/cDNA. A second complex alteration was noted at the junction of intron 2 and exon 3 of *DCK* (Fig. 6*C*). This mutation was also heterozygous and likely responsible for the altered splicing of exon 3. This may

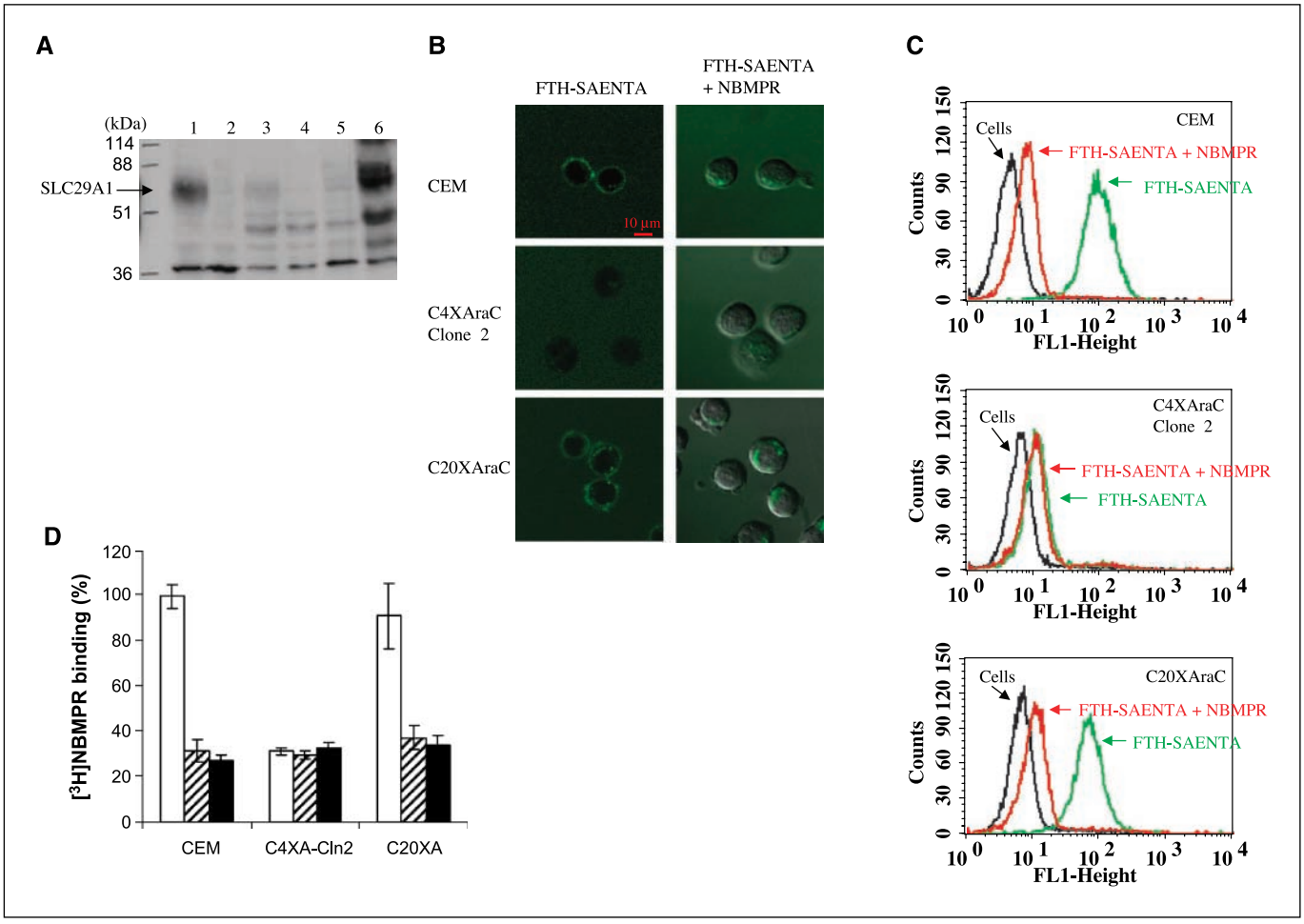

Figure 4. Analysis of hENT1/SLC29A1 protein expression by immunoblotting (*A*), fluorescent staining (*B*), FACS (*C*), and [^{3}H]NBMPR binding (*D*). *A,* immunodetection of hENT1/SLC29A1 protein in CEM and CEM/4×AraC cells using hENT1-specific monoclonal antibodies. *Lanes 1* and *2,* crude membrane from CEM and CEM/4×AraC, respectively; *lanes 3, 4, 5,* and *6,* whole-cell extracts from CEM, CEM/4×AraC, HeLa/vec, and HeLa/ENT1, respectively (50 μg protein per lane). *B,* fluorescent staining with FTH-SAENTA and confocal microscopy of CEM (*top*), CEM/4×AraC, clone #2 (*middle*), and CEM/20×AraC (*bottom*) cells in the absence (*left*) and presence (*right*) of NBMPR. *C,* FACS analysis of CEM (*top*), CEM/4×AraC, clone #2 (*middle*), and CEM/20×AraC (*bottom*) cells. *D,* cell surface [^{3}H]NBMPR binding in CEM, CEM/4×AraC (clone #2), and CEM/20×AraC cells. See Materials and Methods for details.

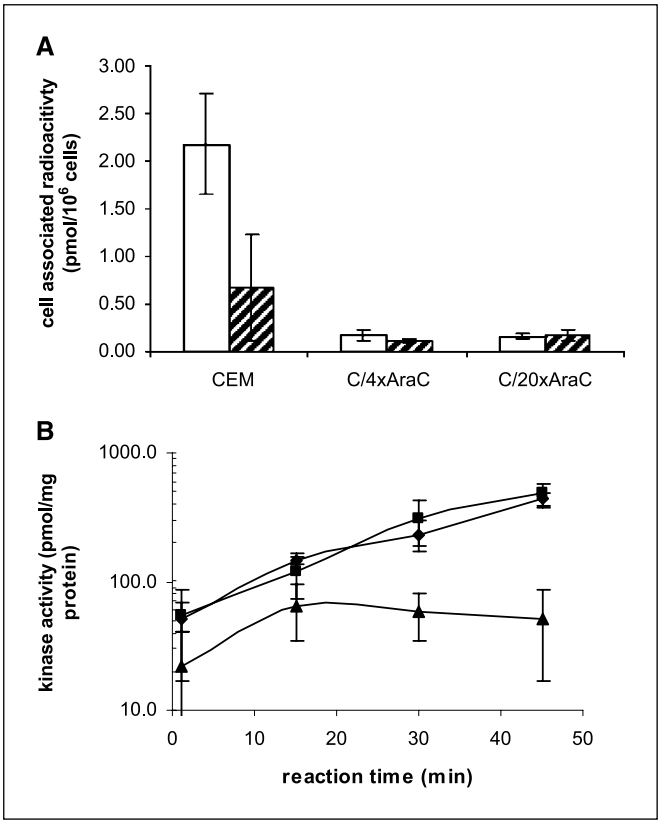

Figure 5. Functional characterization of the drug resistance mechanisms in CEM/4×AraC and CEM/20×AraC cells. *A,* hENT1/SLC29A1-mediated cellular uptake of [^{3}H]AraC was measured by cell-associated radioactivity when cells were incubated with radiolabeled drug under normal (*empty columns*) or ATP depletion (*hatched columns*) conditions, as described in Materials and Methods. *B,* determination of DCK activity in CEM (♦), CEM/4×AraC (■), and CEM.20×AraC (▲) cells, as described in Materials and Methods. The data represent the means of at least three experiments; *bars,* SDs.

have resulted in the 22-bp insertion detected in the cDNA. It is noteworthy that both types of mutations were present in heterozygous fashion at genomic as well as cDNA levels. These results suggested that impaired DCK protein function was responsible for AraC resistance in CEM/20×AraC cells.

Discussion

In the present study, an AraC resistant cell line, CEM/4×AraC, was developed by continuous exposure of the CEM cell line to low concentrations of AraC. Selection of this cell population required several months of continuous culturing in the drug. CEM/4×AraC cells were then subcultured in increasing concentration of AraC until a second population of highly drug resistant cells (CEM/20×AraC) was isolated and stably passaged in the presence of the drug. The mechanism underlying drug resistance in these two cell lines was investigated at the molecular level. The early recognition that the drug resistance profiles of each population exhibited significant overlap, yet were distinct with respect to 5-fluorouridine and 5-fluoro-2′-deoxyuridine (in which the 20× line retained susceptibility compared with the 4× line), indicated that the two cell populations may exhibit different mechanisms of resistance.

Extensive molecular analyses showed that AraC resistance in CEM/4×AraC cells was caused by a complete loss of function of hENT1/SLC29A1, the nucleoside transporter used by AraC as a fraudulent substrate to enter cells. These results are based on the identification of obvious loss-of-function mutations in the *SLC29A1* gene both at the cDNA and genomic levels and were phenotypically translated as loss of protein expression detected by immunoblotting and flow cytometry, lack of binding of known hENT1/SLC29A1 ligands, drastically reduced uptake of radioactive AraC, and cellular cross-resistance to other cytotoxic nucleoside drugs. The observation that the two mutations were found as heterozygotes in the CEM/4×AraC cell population while no full-length wild-type cDNA was produced suggested that each *SLC29A1* gene copy had been sequentially inactivated during drug selection. This mechanism would imply that a reduction of 50% in activity of hENT1/SLC29A1 was sufficient to confer a selective growth advantage in medium containing low levels of the drug (near IC_{50} values). Therefore, it is tempting to speculate that silencing of a single copy of the *SLC29A1* gene in leukemic cells may provide significant cellular resistance and concomitant growth advantage during treatment with AraC. Such biologically relevant silencing may be difficult to detect *in vivo*. Previous studies reported that lack of mRNA and/or protein expression of hENT1/SLC29A1 is highly correlated with cellular resistance to AraC and its close relative, gemcitabine, in both *in vitro* selected drug-resistant cell lines and patients suffering from AML or mantle cell lymphoma (14, 16, 38–41). Conversely, transfection of *SLC29A1* cDNA into otherwise hENT1-deficient cells sensitizes cells to AraC cytotoxicity (38). These studies support the contention that inactivation of hENT1/SLC29A1 may cause cellular resistance to nucleoside analogue drugs, not only in the ALL cells tested here but also in unrelated tumor cell types. Indeed, different tumor cell types have been shown to rely on the same molecular mechanism to achieve resistance to cytotoxic drugs *in vitro* and *in vivo*. A typical example is the overexpression of multidrug transporters MDR1 (ABCB1) and MRP1 (ABCC1; for reviews, see refs. 42, 43). Importantly, the present study is a first example of a loss-of-function mutation in the *SLC29A1* gene that causes cellular resistance to AraC.

The second cell population CEM/20×AraC, loosely derived from the 4× cell line by growth in increasing drug concentration, displayed a mechanism of AraC resistance distinct from that found in the 4× cells. Indeed, hENT1/SLC29A1 function was normal in CEM/20×AraC cells, including the absence of mutations in the gene, presence at the cell surface of a protein that could bind known hENT1/SLC29A1 ligands and capacity to transport uridine. Instead, CEM/20×AraC cells were found to carry obvious loss-of-function mutations in the *DCK* gene which is absolutely required for phosphorylation of AraC, a process necessary for AraC-mediated inhibition of RNA and DNA synthesis. The two mutations identified were heterozygous on each of the *DCK* alleles in the CEM/20×AraC cells, again suggesting sequential inactivation of the *DCK* gene during selection for high-level resistance to AraC. This in turn supports the notion that partial (50%) loss of DCK function may be sufficient to cause clinically relevant AraC resistance. Indeed, decreased DCK expression has been associated with increased AraC resistance in the later the phase of drug selection in an *in vitro* selected human B leukemia cell line (18).

Both AraC-resistant cell lines displayed reduced levels of AraC accumulation. In CEM/4×AraC, mutations in the *SLC29A1* gene blocked cellular uptake of AraC and of other nucleoside analogue drugs, establishing a causal relationship with cellular resistance to these drugs. In the CEM/20×AraC cell line, loss-of-function

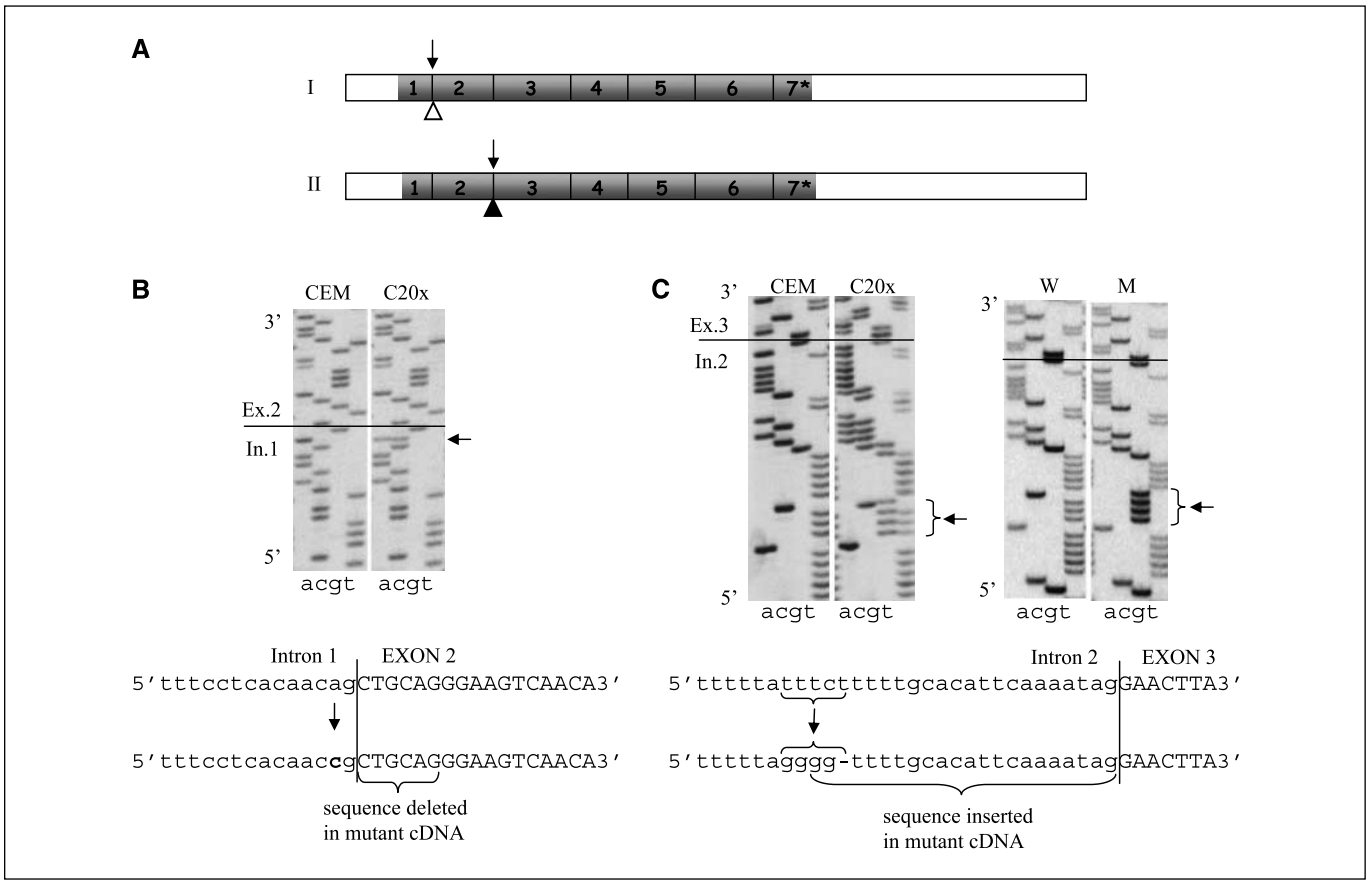

Figure 6. Identification of *DCK* mutations in CEM/20×AraC cells. *A,* schematic representation of two major types of mutations found in cloned full-length coding cDNA (*shaded region*) from CEM/20×AraC. *Type I,* a 6-bp deletion (Δ) at the beginning of exon 2 (*top*); *type II,* a 22-bp insertion (▲) at the beginning of exon 3 (*bottom*). *B,* autoradiographs of [^{33}P]dATP labeled DNA sequencing gel (*top*) and the deduced DNA sequences (*bottom*) of the DCK genomic DNA from CEM (*left*) and CEM/20×AraC (*right*), respectively, in the region of type I mutation. *C,* autoradiograph of [^{33}P]dATP labeled DNA sequencing gels (*top*) and their deduced DNA sequences (*bottom*) of the DCK genomic DNA from CEM and CEM/20×AraC, respectively, in the region of type II mutation. *Left,* sequencing gel of direct genomic PCR products; *right,* sequencing gel of cloned genomic PCR products, showing both wild-type and mutant allele sequences. The positions of mutated residues are indicated by arrows. Boundaries between intron and exons are indicated by lines. Sequences that were deleted or inserted in the mutated DCK cDNA are indicated.

mutations in the *DCK* gene explained resistance to AraC and other nucleoside analogue drugs (e.g., gemcitabine) that are substrates for this enzyme and hence are not phosphorylated in the resistant line. Although these nucleoside analogue drugs can enter cells via a functional hENT1/SLC29A1 protein, they may exit cells by the same route in the absence of phosphorylation due to the equilibrative nature of the transporter. On the other hand, 5-fluorouridine and 5-fluoro-2′-deoxyuridine are not substrates for DCK, can be phosphorylated by other nucleoside kinases, such as uridine kinase, and thus remain cytotoxic to the CEM/20×AraC cells.

Functional studies and sequence analysis of archival samples corresponding to mass populations of CEM stocks frozen at different stages of drug selection has suggested the following scenario for the emergence of AraC resistance in the two CEM cell lines reported herein. The first AraC-selected cell line, CEM/4×AraC, was probably a mixed population, consisting of a large majority of cells bearing *SLC29A1* mutations, and a much smaller number of cells bearing *DCK* mutations (but wild type for *SLC29A1*). Loss of *SLC29A1* function initially imparted low-level resistance to AraC in 4×AraC cells. We speculate that loss of *DCK* function conferred higher level of resistance to AraC than that caused by loss of *SLC29A1* function. Subsequent selection of CEM/4×AraC cells in higher concentrations of AraC (e.g., 20× IC_{50}) caused an expansion of the $DCK^{-/-}$ cells. Further passages and/or subcloning to generate CEM/20×AraC yielded a population of resistant cells highly enriched in $DCK^{-/-}$ cells and devoid of $SLC29A1^{-/-}$ cells. To test this hypothesis, we used an archival early specimen of CEM/4×AraC cells and passaged it for a period of 3 months in 4× IC_{50} of AraC, and each month, a sample was analyzed by FACS for FTH-SAENTA binding (Supplementary Fig. S1) as an indication of hENT1/SLC29A1 surface expression. Over this period, we observed a progressive shift from a population that expressed little hENT1/SLC29A1 to a population that expressed robust amounts, consistent with the notion that the culture was being taken over by a subpopulation of highly resistant DCK-negative cells.

DCK mutations have been previously associated with high levels of AraC resistance in other drug selected cell lines (44, 45). Conversely, introduction of *DCK* cDNA into the $DCK^{-/-}$ cells increased cellular sensitivity to AraC and other nucleoside analogue drugs (46–48). In addition, alternatively spliced *DCK* mRNAs have been detected in leukemic blasts from patients with resistant AML but not in sensitive AML, suggesting that these inactive *DCK* mRNAs might play a role in AraC resistance *in vivo*

(49). These results are consistent with our findings in the CEM/20×AraC cells.

Overall, our results clearly point at hENT1/SLC29A1 and DCK as critical players in the emergence of AraC resistance in tumor cells, in general, and in leukemic cells, in particular. Moreover, these findings *in vitro* have obvious implications for the parallel search of other mutations in these two genes and in members of the same pathway that can be associated with AraC resistance *in vivo*.

Acknowledgments

Received 9/24/2007; revised 12/13/2007; accepted 1/11/2008.

Grant support: This study was made possible by a generous gift from the Lynn P. Mackay Memorial Fund to P. Gros. P. Gros is a James McGill Professor of Biochemistry. C.E. Cass is the Canada Research Chair in Oncology, and work in her laboratory is supported by a grant from the National Cancer Institute of Canada.

The costs of publication of this article were defrayed in part by the payment of page charges. This article must therefore be hereby marked *advertisement* in accordance with 18 U.S.C. Section 1734 solely to indicate this fact.

References

1. Thomas X, Dombret H. Timed-sequential chemotherapy as induction and/or consolidation regimen for younger adults with acute myelogenous leukemia. Hematology 2007;12:15–28.
2. Tsurumi H, Kanemura N, Hara T, et al. Therapeutic strategy of untreated *de novo* acute myeloid leukemia in the elderly: the efficacy of continuous drip infusion with low dose cytarabine and etoposide. J Cancer Res Clin Oncol 2007;133:547–53.
3. Kern W, Estey EH. High-dose cytosine arabinoside in the treatment of acute myeloid leukemia: review of three randomized trials. Cancer 2006;107:116–24.
4. Tedeschi A, Montillo M, Strocchi E, et al. High-dose idarubicin in combination with AraC in patients with relapsed or refractory acute lymphoblastic leukemia: a pharmacokinetic and clinical study. Cancer Chemother Pharmacol 2007;59:771–9.
5. Candoni A, Michelutti A, Simeone E, Damiani D, Baccarani M, Fanin R. Efficacy of liposomal daunorubicin and cytarabine as reinduction chemotherapy in relapsed acute lymphoblastic leukaemia despite expression of multidrug resistance-related proteins. Eur J Haematol 2006;77:293–9.
6. Giebel S, Krawczyk-Kulis M, Adamczyk-Cioch M, et al. Fludarabine, cytarabine, and mitoxantrone (FLAM) for the treatment of relapsed and refractory adult acute lymphoblastic leukemia. A phase study by the Polish Adult Leukemia Group (PALG). Ann Hematol 2006;85:717–22.
7. Oki Y, Ogura M, Kato H, et al. Phase II study of a salvage regimen using cyclophosphamide, high-dose cytarabine, dexamethasone, etoposide, and rituximab in patients with relapsed or refractory B-cell non-Hodgkin's lymphoma. Cancer Sci. Epub 2007 Nov 7.
8. Jo JC, Kang BW, Jang G, et al. BEAC or BEAM high-dose chemotherapy followed by autologous stem cell transplantation in non-Hodgkin's lymphoma patients: comparative analysis of efficacy and toxicity. Ann Hematol. Epub 2007 Aug 21.
9. Mey UJ, Orlopp KS, Flieger D, et al. Dexamethasone, high-dose cytarabine, and cisplatin in combination with rituximab as salvage treatment for patients with relapsed or refractory aggressive non-Hodgkin's lymphoma. Cancer Invest 2006;24:593–600.
10. Lassaletta A, Perez-Olleros P, Scaglione C, et al. Successful treatment of intracranial ependymoma with leptomeningeal spread with systemic chemotherapy and intrathecal liposomal cytarabine in a two-year-old child. J Neurooncol 2007;83:303–6.
11. Ravindranath Y, Chang M, Steuber CP, et al. Pediatric Oncology Group (POG) studies of acute myeloid leukemia (AML): a review of four consecutive childhood AML trials conducted between 1981 and 2000. Leukemia 2005;19:2101–16.
12. Liang DC, Chan TT, Lin KH, et al. Improved treatment results for childhood acute myeloid leukemia in Taiwan. Leukemia 2006;20:136–41.
13. Damaraju VL, Damaraju S, Young JD, et al. Nucleoside anticancer drugs: the role of nucleoside transporters in resistance to cancer chemotherapy. Oncogene 2003;22:7524–36.
14. Hubeek I, Stam RW, Peters GJ, et al. The human equilibrative nucleoside transporter 1 mediates *in vitro* cytarabine sensitivity in childhood acute myeloid leukaemia. Br J Cancer 2005;93:1388–94.
15. Sarkar M, Han T, Damaraju V, Carpenter P, Cass CE, Agarwal RP. Cytosine arabinoside affects multiple cellular factors and induces drug resistance in human lymphoid cells. Biochem Pharmacol 2005;70:426–32.
16. Stam RW, den Boer ML, Meijerink JP, et al. Differential mRNA expression of AraC-metabolizing enzymes explains AraC sensitivity in MLL gene-rearranged infant acute lymphoblastic leukemia. Blood 2003;101:1270–6.
17. Zhang J VF, King KM, Baldwin SA, Young JD, Cass CE. The role of nucleoside transporters in cancer chemotherapy with nucleoside drugs. Cancer Metastasis Rev 2007;26:85–110.
18. Kanno S, Hiura T, Ohtake T, et al. Characterization of resistance to cytosine arabinoside (AraC) in NALM-6 human B leukemia cells. Clin Chim Acta 2007;377:144–9.
19. Achiwa H, Oguri T, Sato S, Maeda H, Niimi T, Ueda R. Determinants of sensitivity and resistance to gemcitabine: the roles of human equilibrative nucleoside transporter 1 and deoxycytidine kinase in non-small cell lung cancer. Cancer Sci 2004;95:753–7.
20. Osato DH, Huang CC, Kawamoto M, et al. Functional characterization in yeast of genetic variants in the human equilibrative nucleoside transporter, ENT1. Pharmacogenetics 2003;13:297–301.
21. Kim SR, Saito Y, Maekawa K, et al. Thirty novel genetic variations in the SLC29A1 gene encoding human equilibrative nucleoside transporter 1 (hENT1). Drug Metab Pharmacokinet 2006;21:248–56.
22. Myers SN, Goyal RK, Roy JD, Fairfull LD, Wilson JW, Ferrell RE. Functional single nucleotide polymorphism haplotypes in the human equilibrative nucleoside transporter 1. Pharmacogenet Genom 2006;16:315–20.
23. Momparler RL, Laliberte J, Eliopoulos N, Beausejour C, Cournoyer D. Transfection of murine fibroblast cells with human cytidine deaminase cDNA confers resistance to cytosine arabinoside. Anticancer Drugs 1996;7:266–74.
24. Schroder JK, Kirch C, Flasshove M, et al. Constitutive overexpression of the cytidine deaminase gene confers resistance to cytosine arabinoside *in vitro*. Leukemia 1996;10:1919–24.
25. Neff T, Blau CA. Forced expression of cytidine deaminase confers resistance to cytosine arabinoside and gemcitabine. Exp Hematol 1996;24:1340–6.
26. Galmarini CM, Graham K, Thomas X, et al. Expression of high Km 5′-nucleotidase in leukemic blasts is an independent prognostic factor in adults with acute myeloid leukemia. Blood 2001;98:1922–6.
27. Galmarini CM, Thomas X, Calvo F, et al. Potential mechanisms of resistance to cytarabine in AML patients. Leuk Res 2002;26:621–9.
28. Jordheim LP, Guittet O, Lepoivre M, Galmarini CM, Dumontet C. Increased expression of the large subunit of ribonucleotide reductase is involved in resistance to gemcitabine in human mammary adenocarcinoma cells. Mol Cancer Ther 2005;4:1268–76.
29. Davidson JD, Ma L, Flagella M, Geeganage S, Gelbert LM, Slapak CA. An increase in the expression of ribonucleotide reductase large subunit 1 is associated with gemcitabine resistance in non-small cell lung cancer cell lines. Cancer Res 2004;64:3761–6.
30. Mansson E, Flordal E, Liliemark J, et al. Down-regulation of deoxycytidine kinase in human leukemic cell lines resistant to cladribine and clofarabine and increased ribonucleotide reductase activity contributes to fludarabine resistance. Biochem Pharmacol 2003;65:237–47.
31. Rooseboom M, Commandeur JN, Vermeulen NP. Enzyme-catalyzed activation of anticancer prodrugs. Pharmacol Rev 2004;56:53–102.
32. Maring JG, Groen HJ, Wachters FM, Uges DR, de Vries EG. Genetic factors influencing pyrimidine-antagonist chemotherapy. Pharmacogenom J 2005;5:226–43.
33. King AE AM, Cass CE, Young JD, Baldwin SA. Nucleoside transporters: from scavengers to novel therapeutic targets. Trends Pharmacol Sci 2006;27:416–25.
34. Jennings LL, Hao C, Cabrita MA, et al. Distinct regional distribution of human equilibrative nucleoside transporter proteins 1 and 2 (hENT1 and hENT2) in the central nervous system. Neuropharmacology 2001;40:722–31.
35. Visser F SL, Damaraju V, Tackaberry T, et al. Residues 334 and 338 in transmembrane segment 8 of human equilibrative nucleoside transporter 1 are important determinants of inhibitor sensitivity, protein folding, and catalytic turnover. J Biol Chem 2007;282:14148–57.
36. Jamieson GP BA, Snook MB, Sawyer WH, Buolamwini JK, Paterson AR, Wiley JS. Flow cytometric quantitation of nucleoside transporter sites on human leukemic cells. Cytometry 1993;14:32–8.
37. Crawford CR, Ng CY, Ullman B, Belt JA. Identification and reconstitution of the nucleoside transporter of CEM human leukemia cells. Biochim Biophys Acta 1990;1024:289–97.
38. Takagaki K, Katsuma S, Kaminishi Y, et al. Gene-expression profiling reveals down-regulation of equilibrative nucleoside transporter 1 (ENT1) in AraC-resistant CCRF-CEM-derived cells. J Biochem (Tokyo) 2004;136:733–40.
39. Mackey JR, Mani RS, Selner M, et al. Functional nucleoside transporters are required for gemcitabine influx and manifestation of toxicity in cancer cell lines. Cancer Res 1998;58:4349–57.
40. Marce S, Molina-Arcas M, Villamor N, et al. Expression of human equilibrative nucleoside transporter 1 (hENT1) and its correlation with gemcitabine uptake and cytotoxicity in mantle cell lymphoma. Haematologica 2006;91:895–902.
41. Galmarini CM. Correlation of hENT1 expression and function with gemcitabine cytotoxicity in mantle cell lymphoma lines and clinical samples. Haematologica 2006;91:866B.
42. Ambudkar SV, Kimchi-Sarfaty C, Sauna ZE, Gottesman MM. P-glycoprotein: from genomics to mechanism. Oncogene 2003;22:7468–85.
43. Szakacs G, Paterson JK, Ludwig JA, Booth-Genthe C, Gottesman MM. Targeting multidrug resistance in cancer. Nat Rev Drug Discov 2006;5:219–34.
44. Stegmann AP, Honders MW, Hagemeijer A, Hoebee B, Willemze R, Landegent JE. *In vitro*-induced resistance to the deoxycytidine analogues cytarabine (AraC) and 5-aza-2′-deoxycytidine (DAC) in a rat model for acute myeloid leukemia is mediated by mutations in the deoxycytidine kinase (dck) gene. Ann Hematol 1995;71:41–7.
45. Stegmann AP, Honders MW, Willemze R, Landegent JE. *De novo* induced mutations in the deoxycytidine kinase (dck) gene in rat leukemic clonal cell lines confer resistance to cytarabine (AraC) and 5-aza-2′-deoxycytidine (DAC). Leukemia 1995;9:1032–8.
46. Stegmann AP, Honders WH, Willemze R, Ruiz van Haperen VW, Landegent JE. Transfection of wild-type deoxycytidine kinase (dck) cDNA into an AraC- and DAC-resistant rat leukemic cell line of clonal origin fully restores drug sensitivity. Blood 1995;85:1188–94.
47. Hapke DM, Stegmann AP, Mitchell BS. Retroviral transfer of deoxycytidine kinase into tumor cell lines enhances nucleoside toxicity. Cancer Res 1996;56:2343–7.
48. Jordheim LP, Galmarini CM, Dumontet C. Gemcitabine resistance due to deoxycytidine kinase deficiency can be reverted by fruitfly deoxynucleoside kinase, DmdNK, in human uterine sarcoma cells. Cancer Chemother Pharmacol 2006;58:547–54.
49. Veuger MJ, Honders MW, Landegent JE, Willemze R, Barge RM. High incidence of alternatively spliced forms of deoxycytidine kinase in patients with resistant acute myeloid leukemia. Blood 2000;96:1517–24.